Science of the Total Environment 758 (2021) 143888

Contents lists available at ScienceDirect

Science of the Total Environment

journal homepage: www.elsevier.com/locate/scitotenv

Attachment of APAM to mineral particles in seawater

Odd Gunnar Brakstad [a,*], Dag Altin [b], Marianne Aas [a], Jørgen Skancke [a], Trond Nordtug [a], Julia Farkas [a]

[a] SINTEF Ocean AS, Environment and New Resources, Trondheim, Norway
[b] BioTrix, Trondheim, Norway

HIGHLIGHTS

- Anionic polyacrylamides (APAM) are used for enhanced oil recovery.
- APAM polymers may be released from produced water at marine conditions.
- Released APAM showed poor attachment to the mineral particles in seawater.
- The data indicated different APAM attachment properties to two types of MPs.
- A small APAM fraction attached to large particles at environmentally relevant concentrations
- The results indicate seawater dilution rather than sedimentation of released APAM.

GRAPHICAL ABSTRACT

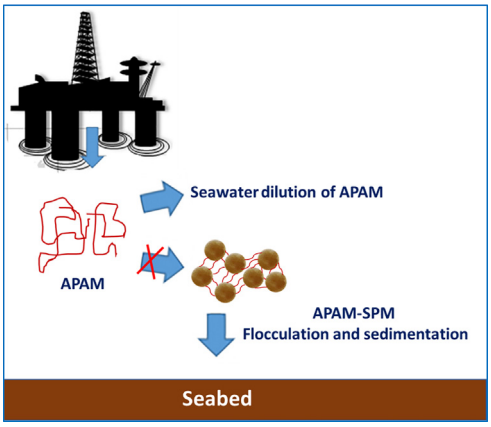

ARTICLE INFO

Article history:
Received 6 October 2020
Received in revised form 18 November 2020
Accepted 18 November 2020
Available online 3 December 2020

Editor: Frederic Coulon

Keywords:
Polymer
APAM
Diatomaceous earth
Kaolin, attachment
Flocculation

ABSTRACT

Polymer injection is used in enhanced oil recovery (EOR) when an oil field ages and the pressure in the reservoir decreases, or for oil fields with heavy oil. By polymer injection, the viscosity of the water injected for pressure support is increased by mixing with a high concentration of a polymer solution. Polymers used in EOR operations are often high molecular weight polyacrylamides, including anionic polyacrylamide (APAM), which may subsequently enter the marine environment with produced water releases. Since seawater (SW) contains mineral particles (MPs) in low concentrations, and polymers like APAM are known to flocculate MPs, we investigated if APAM at different concentrations (0.5–10 mg/L) would attach and flocculate MPs, when these occurred in concentrations relevant for oceanic SW (1 mg/L). Two types of MPs, diatomaceous earth and kaolin, were exposed to fluorescence-tagged APAM (APAM-TAG). A low-energy carousel system with natural seawater (SW) was used for incubation of MPs and APAM-TAG at a temperature relevant for the Norwegian Continental Shelf (13 °C). Attachment to MPs and aggregates of these were analysed by fluorometry and fluorescence microscopy. Particle analyses showed that only minor fractions of the MPs aggregated. When samples were separated in steel filter with a mesh size of 20 μm, APAM-TAG was mainly measured in the flow-through fraction (<20 μm), and the results therefore showed that the polymer mainly remained in the water-phase, or was attached to small particles (<20 μm). For the small fraction of APAM attaching to aggregated MPs, attraction to kaolin was higher than to diatomaceous earth, and fluorescence microscopy analyses confirmed the presence of fluorescent particles at the higher APAM concentrations. MPs at concentrations relevant for oceanic SW are therefore not expected to significantly contribute to sedimentation of APAM dissolved in the water column.

* Corresponding author at: SINTEF Ocean AS, Postboks 4762 Torgarden, 7465 Trondheim, Norway.
E-mail address: odd.g.brakstad@sintef.no (O.G. Brakstad).

https://doi.org/10.1016/j.scitotenv.2020.143888

1. Introduction

High molecular weight polyacrylamides (PAMs) are widely used in many industrial processes, for instance in flocculation and complexation of particulate matter. These polymers, including anionic polyacrylamide (APAM), have also been introduced for polymer flooding in enhanced oil recovery (EOR) operations. APAM increases the viscosity of the displacement/flooding water, resulting in effects on fractional flow, decrease of water/oil mobility ratio, and diversion of injected water from zones that have been swept (Needham and Doe, 1987). Polymer flooding with APAM has been implemented in full-scale in the Daqing reservoir in China in 1996 (Wang et al., 2009) and have also been tested for offshore reservoirs in a pilot study at the Dalia field located off-shore Angola (Morel et al., 2015). Reliable analytical methods for APAM measurements have high detection limits, and data on environmental concentrations are therefore rare. A report from the Shengli Oilfield in China reported 170 mg/L polymer (named residual hydrolysed PAM) in raw produced water (Zhang et al., 2010), but in the marine water column, polymer concentrations will be rapidly decreased after release.

In offshore EOR processes, APAM will follow the produced water and can thus enter the marine environment with produced water discharges. During EOR operations, large quantities of polymers will be used, and since these high molecular weight PAMs show negligible biodegradation (El-Mamouni et al., 2002), their environmental transport and fate need to be better understood in order to assess potential impacts of the polymer in the marine environment. The fate and impacts of APAM on potentially exposed habitats/ecosystems will depend on the local environmental conditions, particularly on the presence of particulate matter that can interact with dissolved polymer. The distribution of APAM in the water column between soluble and particulate phases is largely unknown, although a recent study reported insignificant interactions between APAM and live or dead algal material (Brakstad et al., 2020). Since APAM is highly water-soluble, the polymer will be rapidly diluted after release to seawater (SW), but potential flocculation with suspended particulate material (SPM) may result in seabed sedimentation. APAM may flocculate mineral particles (MPs) like kaolin. Although both APAM and kaolin have negative net charges, adsorption still occurs through hydrogen bonding between the silanol and aluminol OH groups at the particle surface and the polymer's primary amide functional groups. Electrostatic repulsions between the negatively charged polymer and kaolinite surfaces allow extensions of the anionic polymer molecules, forming loops and tails. Polymer bridging occurs to a greater extent with less particle adsorption. This is associated with larger open-structure flocs with less resistance to compression loads and subsequent production of compact sediments (Nasser and James, 2006).

In SW, containing high concentrations of monovalent and multivalent cations, negatively charged polymers like APAM will become more compressed than in low-salinity solutions, since SW cations (e.g. Na^+ and Ca^{2+}) will result in increased polymer packing by shielding and crosslinking of repulsive anions (Zhang et al., 2008). Most particulate materials in SW have net negative charges (Neihof and Loeb, 1972), and the adsorption to the negatively charged APAM occurs through hydrogen bonding at the particle surface, and to the polymer's primary amide functional groups. Saline conditions have also been shown to enhance flocculation of mineral tailings compared to freshwater conditions, since cations in the salts reduced electrostatic repulsions between the negatively charged solid particles and negatively charged polymer flocculants, resulting in more effective polymer bridging interactions (Ji et al., 2013).

SPM in the marine water column may be of terrigenous and marine sources, with more than 80% of coastal-zone sediments originating from terrestrial sources, with rivers as the predominant pathway of terrigenous sediment transport to the sea (Milliman and Syvitski, 1992; Garrison, 2012). In polar regions, glaciers are an important vector for sediment and particle transport. Particles of marine origin may include marine biogenic particles and particles forming by chemical precipitation (e.g. of salts during evaporation processes). Biogenic sediments contain 30% or more grains of biological origin, mostly calcium carbonate (calcite; aragonite) oozes produced by coccolithophoridae and/or foraminifera (predominant in shallower and warmer water) or opalline silica from diatoms, radiolaria shells and siliceous sponges (deeper and colder water). Despite high dissolution rates of biological carbonates, biogenic sediments are the dominant sediment type of deep ocean floors. While SPM in offshore waters are predominantly of organic origin (phytoplankton, biomass debris), inorganic particulate materials (e.g. silt, clay and sand) are the dominating suspended components in inshore waters (Bowers and Binding, 2006; Zhao et al., 2011). SPM concentrations in seawater may vary considerably, from 25 to 100 mg/L in coastal seawater like the Southern North Sea (Fettweis et al., 2007), to average 0.02 to 1 mg/L in ocean seawater, and decreasing with greater depth (Sheldon et al., 1972). The organic content in SPM was shown to range from 6 to 11% in coastal North Sea water (Ferrari et al., 2003), while the organic carbon content in the particulate fractions from samples collected in the Southern Atlantic ocean ranged from 6.5 to 29% (Albuquerque et al., 2014) in this study. The authors reported a strong marine (autochthonous) influence.

Since APAM may flocculate particulate material, more information is needed to determine if low concentrations of the polymer, released with produced water, may attach to SPM in the marine water column. APAM attachment to SPM may cause seabed sedimentation of the polymer, while poor attachment may result in rapid dilution of the water-miscible polymer in the water column. The objective of the study was therefore to determine if APAM released with produced water from offshore oil production can interact with SPM and form polymer-particle aggregates. Such aggregates may increase the rate of polymer sedimentation. Different environmentally realistic concentrations of APAM were used in combinations with SPM concentrations relevant for ocean SW. Two types of SMP were included in the study, opaline silica from diatoms (diatomaceous earth) representing marine particles of biogenic origin, and kaolin representing finely grained clay minerals originating from granite rock.

2. Materials and methods

2.1. Seawater, chemicals and mineral particles

The SW used in the study was collected from a depth of 80 m (close to the seabed) in the local fjord outside the harbour area of Trondheim, Norway (63°26′N, 10°24′E). The SW is transported to the laboratory of SINTEF Ocean though a pipeline system made from polyethylene. The depth of the pipeline inlet is well below the thermocline, securing a stable temperature all the year around. The SW has a salinity of 34‰, and the water source is considered to be non-polluted and not heavily influenced by seasonal variations. The SW passes a sand filter before entering our laboratories, to remove coarse particles. Recent studies showed concentrations of mineral nutrients to be 19 μg/L total-P, 16 μg/L PO_4-P, 130 μg/L NO_2 + NO_3-N, and 3 μg/L NH4-N, and <0.05 mg/L Fe (Brakstad et al., 2015).

Two types of commercially available MPs were included in the study, diatomaceous earth with a reported median volumetric size of 16.2 (± 11.6) μm (Celite 512; Fe_2O_3), and kaolin ($Al_2Si_2O_5(OH)_4$) with a reported median volumetric size of 18.9 (±15.3) μm, both purchased from Sigma-Aldrich. The densities of Celite 512 and kaolin were 2.3 g/cm^3 and 2.65 g/cm^3, respectively, according to information from the supplier.

A fluorescent APAM (200 kDa; lot no. EFO 2109-A, hereafter denoted as 'APAM-TAG') was provided by the polymer producer SNF (SNF, Andrézieux, France), synthesized from acrylamide, acrylamido tertiary butyl sulfonate and a fluorescent monomer as recently described (Brakstad et al., 2020), and with an excitation/emission wavelengths of 396 nm/511 nm. An APAM-TAG stock solution of 5000 mg/L was

prepared in sterile-filtered SW (0.2 μm) by applying 1.0 g APAM-TAG to 200 mL SW by a procedure described by SNF (https://snf.com.au/downloads/Preparation_of_Organic_Polymers_E.pdf). An external calibration curve of APAM-TAG was prepared in sterile-filtered SW. An external fluorometric calibration curve with or without MPs included (1 mg/L Celite 512) showed linearity within the concentration range 0.2 to 10 mg/L of APAM-TAG and negligible interference by MPs at concentrations of 1 mg/L (Supplementary Material 1, Fig. S1).

2.2. Experimental setup

The experiments were conducted in screw-capped polyethylene terephthalate (PET) bottles (1.1 L volume) mounted on a slowly rotating a carousel system (0.75 rpm) (Brakstad et al., 2015; Brakstad et al., 2020). The PET bottles were completely filled with natural SW containing 1 mg/L MPs (Celite 512 or kaolin) and pre-incubated at 13 °C for 10 days on the carousel. The pre-incubation was performed to establish a natural environment of bacterial biofilms on MPs, since bacteria are known to produce extracellular polymeric substances (EPS) when they settle on small particle surfaces as part of biofilm generation (Wang et al., 2002; Chomiak et al., 2014). After 10 days of MP incubation, APAM-TAG was applied from the sterile-filtered stock solution (5000 mg/L) to reach final nominal concentrations (triplicate) of 10 mg/L, 5 mg/L, 2 mg/L, 0.5 mg/L, or without APAM (0 mg/L) (bottles 1 to 15, Table S1, Supplementary Material 2). Bottles without MPs (APAM-TAG in natural SW) were also included (triplicate) to compare with SW without particles (bottles 16–18 in Table S1). Sterilized controls included filtered SW (0.2 μm) pre-incubated for 10 days with MPs, and with subsequent application of 2 mg/L APAM-TAG from a sterile-filtered stock solution (bottles 19–21, Table S1). Additional bottles were incubated for 2 days with fresh MPs (1 mg/L, no pre-incubations) in natural SW with APAM-TAG (2 mg/L) to compare aggregation and polymer attachment when no bacterial biofilms could be established before APAM application (bottle 22–24, Table S1), and as controls without APAM (flasks 25–27, Table S1). Finally, some bottles representing the different treatments (fresh natural SW with 1 mg/L MP and 2 mg/L APAM, pre-incubated SW with MP and subsequent incubation with or without APAM, or pre-incubated SW without MP with subsequent application of APAM) were included for measurements of dissolved oxygen (DO) and for particle analyses by Coulter Counter measurements (bottles 28–31, Table S1). After application of APAM (day 10), all samples were incubated at 13 °C for 2 days on the carousels (0.75 rpm). During incubation with APAM-TAG, the bottles were left with a small headspace (10 mL) to secure turbulence during rotation. Separate and identical experiments were conducted with Celite 512 and kaolin.

2.3. Sampling

After application of APAM-TAG to pre-incubated or fresh SW (see Table S1), samples from incubated bottles were collected for analyses after incubation of 2 days (13 °C). The complete content of each bottle was carefully filtered through steel filters with 20 μm square mesh size (Teichhansel Teichshop/Siebgewebeshop; Bockhorn, Germany) by gravimetric force, as previously described (Netzer et al., 2018; Brakstad et al., 2020). The use of steel filters eliminated the risk of attachment of soluble APAM-TAG to any filter material. The steel filters with particulate materials were placed in EM flasks with 100 mL sterile-filtered (0.2 μm) SW and subjected to orbital shaking for 3 days for detachment of trapped material (>20 μm) from the filters. The detached material was then analysed by fluorometry. Flow-through material (filtrate) passing the steel filter mesh (<20 μm) was measured directly in a fluorometer.

Detached material (10 mL) from some of the steel filters representing different APAM-TAG treatments (0, 0.5, 2, 5 and 10 mg/L) with kaolin, and treatment without MP (2 mg/L APAM-TAG) were used for fluorescence microscopy analyses.

DO, MP concentrations and size distributions were determined in PET-bottles 28–31 (see Table S1) in fresh SW (bottle 28), after 10 days pre-incubation (bottles 29–31), and after 12 days incubation, i.e. 2 days with APAM-TAG (bottles 28–31).

2.4. Analyses

Samples of detached and flow-through materials were analysed in a filter fluorometer (Model TD700, Turner Designs, San Jose, CA, USA) fitted with AT350/50× (Chroma Tech. Corp., Bellows Falls, VT, US) excitation and 450DP65 (Omega Optical, Brattleboro, VT, US) emission filters. The fluorometer was calibrated with a solution of 15 mg/L APAM-TAG to a value of 1000 FSU (arbitrary Fluorescent Signal Units) and corrected for a background fluorescence in sterile-filtered SW. The external calibration curve (Supplementary Material 1, Fig. S1) showed a linear relationship between FSU and APAM-TAG concentration in the range 0.2 to 10 mg/L and negligible interferences of MPs at the concentration used in the experiment (1 mg/L).

Microscopical analyses of detached materials from steel filters were performed under white light or fluorescence microscopy with 20× and 40× objectives in an upright microscope (Nikon Eclipse 90i, Nikon Corp., Japan), as recently described (Brakstad et al., 2020). For white light microscopy, differential interference contrast (DIC) was used, while fluorescence microscopy was performed with a XF10 filter (Omega Optical, Brattleboro, VT, USA), following excitation with a mercury-halide lamp (HPX R 120w/45c, Osram GmbH, Munich, Germany) mounted in an external light source (EL6000, Leica Microsystems, Wetzlar, Germany).

DO was measured to determine SW oxygen saturation during the flocculation experiments with a BOD-probe connected to a dissolved oxygen meter (probe 5905/model 59 m, YSI Inc., Yellow Springs, OH, US) in all samples before filtration through the steel filters.

Particle concentrations and size distributions were determined by Coulter Counter measurements (Beckman Multisizer 4; Beckman Coulter Inc., Brea, CA, U.S.A.), fitted with a 280 μm aperture for measurements of particles with a diameter range of 5.6–100 μm, using sterile-filtered (0.2 μm) SW as electrolyte. Volumetric size distributions and total particle volumes were determined. Total concentrations of MPs by weight (mg/L) were calculated based on the density of the particles (2.3 g/cm^3 for Celite 512 and 2.65 g/cm^3 for kaolin).

Comparison between treatments was determined by ANOVA analyses (GraphPad Prism version 6.0, GraphPad Software, San Diego, CA, USA).

2.5. Other tests

A qualitative flocculation pre-test was performed to determine if the APAM-TAG would settle kaolin in SW. Kaolin (3 g) was applied to a screw-capped Erlenmeyer flasks and wetted with 7 mL $CaCl_2$ from a 1% (wt/vol) solution. APAM-TAG (2 mg/L) in 45 mL SW was applied and the suspension carefully mixed by inverting the closed flasks 3 times. The flasks were left for up to 15 min and settling recorded visually. Controls included a) kaolin without $CaCl_2$ and APAM-TAG in SW, and b) kaolin and $CaCl_2$ in SW without APAM-TAG.

3. Results and discussion

3.1. Particle concentrations and size distributions

Nominal concentrations of MP suspensions (both Celite and kaolin) were approximately 1 mg/L, which is relevant for the particle concentrations in oceanic SW (Sheldon et al., 1972). Measured particle concentrations and median size distributions by Coulter Counter analyses are shown in Table 1. The measured concentrations in the samples were

Table 1
Particle concentrations (mg/L) and median particle sizes (μm) at the start of the pre-incubation (d0), after 10 days of pre-incubation (d10), and after additional 2 days of incubation with 2 mg/L APAM (d12), determined by Coulter Counter analyses. Median sizes are shown with standard deviations of three replicates.

	d0		d10		d12	
	Conc. (mg/L)	Median size (μm)	Conc. (mg/L)	Median size (μm)	Conc. (mg/L)	Median size (μm)
Celite without APAM	1.05	16.2 ± 11.6	0.98	16.5 ± 9.9	1.04	20.5 ± 10.2
Celite with APAM	na[A]	na[A]	na[A]	na[A]	1.05	19.5 ± 11.4
Kaolin without APAM	1.26	18.9 ± 15.3	0.46	21.9 ± 13.9	0.02	27.7 ± 9.6
Kaolin with APAM	na[A]	na[A]	na[A]	na[A]	0.05	27.7 ± 8.9

[A] na, not analysed.

close to the nominal concentrations of 1 mg/L at the start of the experiments, and the particle concentrations remained close to 1 mg/L in the Celite suspensions, with slightly increased median particle size distribution throughout the incubation period. The kaolin concentrations were reduced by more than 90% during the experiment, both in suspensions with and without APAM, and an increasing median particle size distribution of kaolin was measured. However, the particle size distributions of Celite and kaolin did not change significantly during the incubation periods ($P > 0.05$, one-way ANOVA analyses). If kaolin aggregation occurred, large aggregates with sizes outside the Coulter Counter measurement range (>100 μm) may have been formed, explaining the reduced kaolin concentration. Small kaolin particles may therefore aggregate easier than Celite. However, this aggregation was not affected by APAM and may therefore be the result of small surface charge differences between the two types of particles, affecting the electrostatic repulsions between individual particles in the saline environment (Ji et al., 2013). Consequently, APAM concentrations at 10 mg/L and below had no significant impact on MP aggregation.

3.2. APAM distribution between SW and potential MP aggregates

MP aggregation potentials of APAM were observed in a pre-test with high concentrations (58 g/L) of kaolin (Supplemental Material 3, Fig. S2). This qualitative test showed better particle sedimentation in the presence of APAM than without polymer, even at the low concentration of approximately 2 mg/L APAM used in the test. APAM was therefore able to flocculate negatively charged particles in SW at a high particle concentration. The sedimentation was improved by including $CaCl_2$ (Fig. S2), which is a common coagulant used in flocculation tests to reduce repulsive forces between particles by neutralizing surface charges (Gan and Liu, 2008). Despite theoretical charge-related APAM-kaolin repulsion, APAM has been suggested to flocculate kaolin more efficiently than cationic polyacrylamides (Nasser and James, 2006).

According to Stokes Law, sinking velocities decrease with porosity and increase with density. Although Stokes Law is applicable for spherical particles, mesocosm studies of MPs with heterogeneous morphologies have revealed relations between MP size and sinking velocity (Bressac et al., 2012). Aggregates of MPs and APAM may therefore result in polymer sedimentation. Partitioning of APAM between a soluble SW phase and particles >20 μm was determined over a 2-days incubation period following a 10-day pre-incubation period, using steel filters with a 20 μm mesh size for the partitioning. The filter mesh size would result in a flow-through filtrate of mainly soluble APAM and small single particles, while the trapped material included larger particles and aggregates (>20 μm), and presumably with higher densities than particles in the filtrates. The pre-incubation period was included to adapt the Celite and kaolin particles to SW conditions, for instance to accumulate sessile microorganisms on the particle surfaces (Hoppe, 1984). Although a small (8,5%) reduction in SW DO was measured in the experiment with Celite during the 12 days incubation period, DO consumption determined during the experiments was insignificant, indicating no or negligible microbial respiration (Supplementary Material 4, Table S2).

APAM-TAG concentrations in filter-trapped materials with particle size >20 μm and in the filtrates were determined by fluorometry after correcting for the background fluorescence in the SW samples without APAM-TAG. More than 99% of the APAM-TAG was quantified in the filtrates at all APAM-TAG concentrations with Celite, and ≥ 95% with kaolin (Fig. 1). Limited to negligible attachments/interactions of APAM to the large MPs/aggregates were therefore determined. Comparison of fluorescence between treatments with APAM-TAG concentrations of 2 mg/L (pre-treated SW, no MPs, sterilized SW and fresh SW) did not show significant differences ($P > 0.05$; two-way ANOVA analyses). The total calculated APAM-TAG concentrations in the filtrates with natural SW with MPs and APAM were generally slightly lower than the nominal total concentrations (79.3 ± 9.7% of the nominal concentrations, as shown in Fig. 1). However, measured APAM concentrations with both MPs in sterilized SW were close to 2 mg/L APAM (95% to 102% of nominal concentrations). Our findings suggest that the APAM-TAG was associated with the SW soluble phase or with small particles

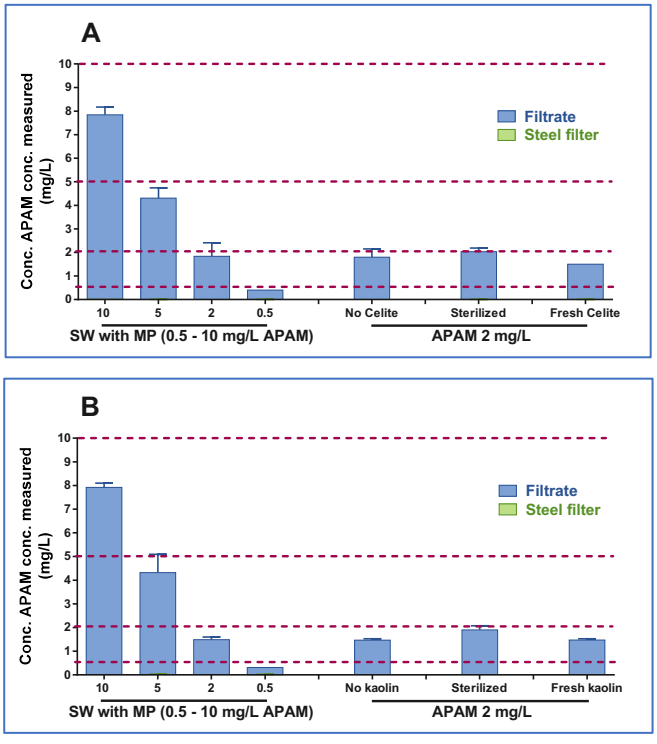

Fig. 1. APAM-TAG concentrations (with standard deviations of three replicates shown as error bars) in material trapped on steel filters and filtrates in experiments with mineral particles (1 mg/L) of Celite 512 (A) or kaolin (B). Experiments were performed with four nominal APAM concentrations (0.5 to 10 mg/L) and MP, with APAM in SW without MP (no Celite or no kaolin), with sterilized APAM and MP suspensions (Sterilized) and with APAM and MPs in fresh SW without previous 10 days pre-incubations (Fresh Celite or kaolin). The concentrations were determined after correcting for fluorescence in samples without APAM-TAG and were calculated by linear regression analyses from the external calibration curve (Supplementary Material 3, Fig. S4). The broken lines represent nominal APAM-TAG concentrations (10 mg/L, 5 mg/L, 2 mg/L and 0.5 mg/L).

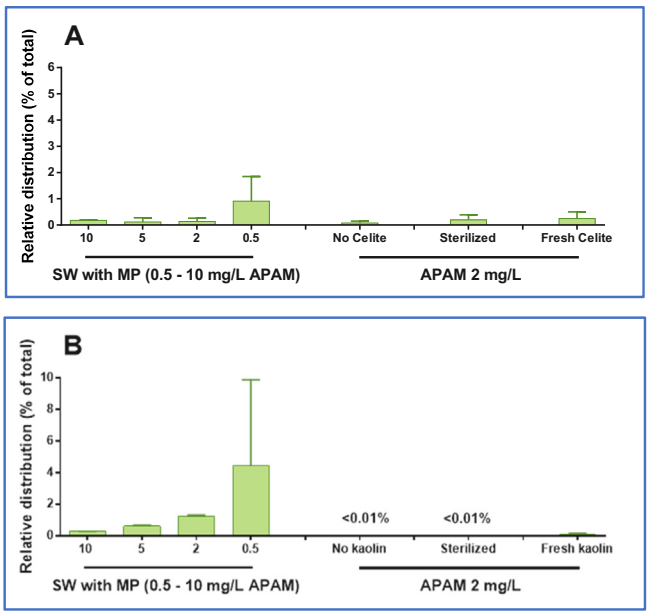

Fig. 2. Relative fraction of APAM-TAG trapped on steel filters, determined as % of total in experiments with Celite (A) and kaolin (B). For further explanation, see Fig. 1.

(<20 μm) present in the seawater. Since the particle analyses showed median sizes close to 20 μm (Table 1), and visual observations only indicated minor to moderate aggregation, a part of the MPs probably ended up in the filtrates. However, since particle analyses implied some aggregation at the end of the experiments, particularly with kaolin (median particle size 28 μm after 12 days of incubation; Table 1), considerable portions of the MPs should be trapped on the filters. Closer examination showed that low fractions of APAM-TAG were trapped on the steel filters, although the results differed between the experiment with Celite and kaolin (Fig. 2). While APAM-TAG in filter-trapped material with Celite was negligible (<1% of total; Fig. 2A), the fraction of trapped APAM-TAG was higher with kaolin (≤5%; Fig. 2B). Further, the phase distribution in the kaolin experiments differed between normal and filter-sterilized SW, since trapped APAM-TAG in sterilized SW was lower than the analytical detection limit. Our data indicated that any APAM attachment to Celite is mainly caused by physical processes, since results in normal and sterilized SW did not differ. In contrast, attachment in kaolin suspensions differed between the particulate phase from sterilized and normal SW exposures, as well as between pre-incubated and fresh SW exposures, indicating that adaption of kaolin to SW increased fluorescence in the particulate phase. This could be explained by a) more APAM-TAG is trapped in kaolin than in Celite suspensions, due to the larger median kaolin particle sizes (Table 1); b) SW microbes attached to kaolin during pre-incubation aided in APAM-TAG attachment; or c) fluorescence with kaolin suspensions was the result of attached bacteria during pre-incubations producing extracellular polymeric substances (EPS). We recently showed that algal transparent exopolymer particles (TEP) caused fluorescence interfering with the APAM-TAG fluorescence (Brakstad et al., 2020), and bacterial EPS materials may also be expected to interfere. Bacteria are known to produce EPS when they settle on small particle surfaces as part of biofilm generation (Wang et al., 2002; Chomiak et al., 2014).

To further investigate the fluorescence of trapped material from the steel filters, desorbed materials from the filters were examined by white light and fluorescence microscopy. Comparison of images from DIC-enhanced white light and blue fluorescence microscopy showed that fluorescent particles were observed at the higher APAM-TAG concentrations (10 mg/L and 5 mg/L), and the fluorescence was associated the particles observed by white light microscopy (Fig. 3). No fluorescence was observed in control images without APAM-TAG and at the lower APAM-TAG observations, with the latter probably due to too low concentrations for visual detection. These results therefore indicate that the blue fluorescence derived from the APAM-TAG and not from EPS produced by microbes attached to the kaolin particles.

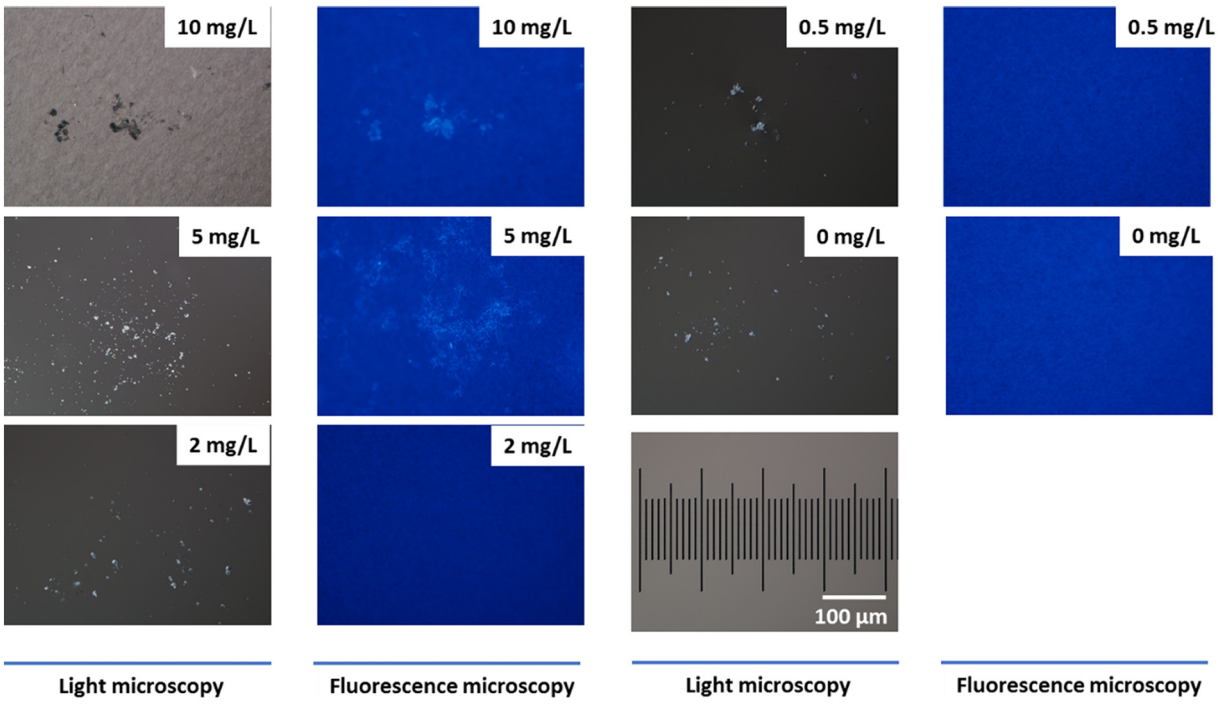

Fig. 3. DIC-enhances white light and blue fluorescence microscopy of desorbed material from steel filters after incubation with kaolin (1 mg/L) and different concentrations of APAM-TAG (0.5 to 10 mg/L), as well as a control sample without APAM-TAG (0 mg/L) and 1 mg/L kaolin. A scalebar is included.

4. Conclusions

The results of our study showed that APAM was associated with the filtrate SW phase, representing the soluble polymer and small particles (<20 μm), rather than the filter-trapped phase consisting of large particles or aggregates. However, a small fraction of the polymer (≤5%) attached to kaolin particles >20 μm, particularly at the more environmentally relevant lower APAM concentrations, in which the polymer concentration was not in quantitative excess compared to MP concentrations. While APAM attachment to large MPs and aggregates may result in sedimentation, attachment to smaller MPs will to a greater extent be entrained in ocean current systems. The results also indicated different attachment properties of two types of MPs. While APAM attachment to diatomaceous earth (Celite 512) seemed to be associated with the inherent surface properties of the particles, attachment to kaolin seemed to be more related to microbial colonization of the particles prior to contact with APAM, as shown by comparison of experiments in normal and sterilized SW. We therefore suggest that APAM released to the marine environment with produced water will primarily be diluted in the water column as water-miscible polymer. Thus, since the SPMs showed poor aggregation properties, any potential sedimentation of APAM will probably be related to particles like marine snow involving TEP/EPS-producing marine organisms like phytoplankton and bacteria. However, recent studies showed that APAM attached poorly also to phytoplankton aggregates > 20 μm. (Brakstad et al., 2020).

The results from analyses by fluorometry and microscopical observations further showed that a combination of low MP concentration in oceanic SW, and rapid dilution of APAM after release, will not result in extensive MP flocculation and sedimentation. Fractions of MPs <20 μm could still be present in the filtrates, and possible polymer attachment to small-size MPs may therefore occur. However, these small-size particles are probably too small for rapid sedimentation and will mainly the dispersed in the water-column by prevailing currents.

CRediT authorship contribution statement

Odd Gunnar Brakstad: Conceptualization, Data curation, Methodology, Supervision, Validation, Writing – original draft, Writing – review & editing. **Dag Altin:** Conceptualization, Data curation, Formal analysis, Methodology, Writing – original draft. **Marianne Aas:** Conceptualization, Data curation. **Jørgen Skancke:** Conceptualization, Writing – original draft, Funding acquisition, Project administration. **Trond Nordtug:** Conceptualization, Data curation, Writing – original draft, Writing – review & editing. **Julia Farkas:** Writing – original draft, Writing – review & editing.

Declaration of competing interest

The authors declare that they have no known competing financial interests or personal relationships that could have appeared to influence the work reported in this paper.

Acknowledgments

This project was financed by Equinor Energy AS. SNF provided the tagged polymers used in the exposure and flocculation experiments. We would like to thank Marianne Aune Molid for technical assistance during the experiments.

Appendix A. Supplementary data

Supplementary data to this article can be found online at https://doi.org/10.1016/j.scitotenv.2020.143888.

References

Albuquerque, A.L.S., Belem, A.L., Zuluaga, F.J., Cordeiro, L.G., Mendoza, U., Knoppers, B.A., Gurgel, M.H., Meyers, P.A., Capilla, R., 2014. Particle fluxes and bulk geochemical characterization of the Cabo Frio upwelling system in Southeastern Brazil: sediment trap experiments between Spring 2010 and Summer 2012. An. Acad. Bras. Cienc. 86, 601–620.

Bowers, D., Binding, C., 2006. The optical properties of mineral suspended particles: a review and synthesis. Estuar. Coast. Shelf Sci. 67, 219–230.

Brakstad, O.G., Nordtug, T., Throne-Holst, M., 2015. Biodegradation of dispersed Macondo oil in seawater at low temperature and different oil droplet sizes. Mar. Pollut. Bull. 93, 144–152.

Brakstad, O.G., Altin, D., Davies, E.J., Aas, M., Nordtug, T., 2020. Interaction between microalgae, marine snow and anionic polyacrylamide APAM at marine conditions. Sci. Tot. Environ. 705, 135950.

Bressac, M., Guieu, C., Doxaran, D., Bourrin, F., Obolensky, G., Grisoni, J.-M., 2012. A mesocosm experiment coupled with optical measurements to assess the fate and sinking of atmospheric particles in clear oligotrophic waters. Geo-Marine Lett. 32, 153–164.

Chomiak, A., Sinnet, B., Derlon, N., Morgenroth, E., 2014. Inorganic particles increase biofilm heterogeneity and enhance permeate flux. Water Res. 64, 177–186.

El-Mamouni, R., Frigon, J.-C., Hawari, J., Marroni, D., Guiot, S.R., 2002. Combining photolysis and bioprocesses for mineralization of high molecular weight polyacrylamides. Biodegradation 13, 221–227.

Ferrari, G.M., Bo, F.G., Babin, M., 2003. Geo-chemical and optical characterizations of suspended matter in European coastal waters. Estuar. Coast. Shelf Sci. 57, 17–24.

Fettweis, M., Nechad, B., Van den Eynde, D., 2007. An estimate of the suspended particulate matter (SPM) transport in the southern North Sea using SeaWiFS images, in situ measurements and numerical model results. Cont. Shelf Res. 27, 1568–1583.

Gan, W., Liu, Q., 2008. Coagulation of bitumen with kaolinite in aqueous solutions containing Ca^{2+}, Mg^{2+} and Fe^{3+}: effect of citric acid. J. Colloid Interface Sci. 324, 85–91.

Garrison, T.S., 2012. Essentials of Oceanography. Brooks/Cole, Belmont, USA 496 pages.

Hoppe, H.-G., 1984. Attachment of bacteria: advantage or disadvantage for survival in the aquatic environment. In: Marshal, K.C. (Ed.), Microbial Adhesion and Aggregation. Springer, Berlin, pp. 283–301.

Ji, Y., Lu, Q., Liu, Q., Zeng, H., 2013. Effect of solution salinity on settling of mineral tailings by polymer flocculants. Colloids and Surfaces A: Physicochem. Engineer. Aspects 430, 29–38.

Milliman, J.D., Syvitski, J.P., 1992. Geomorphic/tectonic control of sediment discharge to the ocean: the importance of small mountainous rivers. J. Geol. 100, 525–544.

Morel, D., Zaugg, E., Jouenne, S., Danquigny, J., Cordelier, P., 2015. Dalia/Camelia Polymer Injection in Deep Offshore Field Angola Learnings and In Situ Polymer Sampling Results. SPE Asia Pacific Enhanced Oil Recovery Conference, Society of Petroleum Engineers.

Nasser, M., James, A., 2006. The effect of polyacrylamide charge density and molecular weight on the flocculation and sedimentation behaviour of kaolinite suspensions. Sep. Purific. Technol. 52, 241–252.

Needham, R.B., Doe, P.H., 1987. Polymer flooding review. J. Petrol. Technol. 39, 1,503–501,507.

Neihof, R.A., Loeb, G.I., 1972. The surface charge of particulate matter in seawater. Limnol. Oceanograph. 17, 7–16.

Netzer, R., Henry, I.A., Ribicic, D., Wibberg, D., Brönner, U., Brakstad, O.G., 2018. Petroleum hydrocarbon and microbial community structure successions in marine oil-related aggregates associated with diatoms relevant for Arctic conditions. Mar. Pollut. Bull. 135, 759–768.

Sheldon, R., Prakash, A., Sutcliffe Jr., W., 1972. The size distribution of particles in the ocean 1. Limnol. Oceanograph. 17, 327–340.

Wang, W., Wang, W., Zhang, X., Wang, D., 2002. Adsorption of p-chlorophenol by biofilm components. Water Res. 36, 551–560.

Wang, D., Dong, H., Lv, C., Fu, X., Nie, J., 2009. Review of practical experience by polymer flooding at Daqing. SPE Reservoir Eval. Engineer. 12, 470–476.

Zhang, Q., Zhou, J.-s, Zhai, Y.-a, Liu, F.-q, Gao, G., 2008. Effect of salt solutions on chain structure of partially hydrolyzed polyacrylamide. J. Central South Univ. Technol. 15, 80–83.

Zhang, Y., Gao, B., Lu, L., Yue, Q., Wang, Q., Jia, Y., 2010. Treatment of produced water from polymer flooding in oil production by the combined method of hydrolysis acidification-dynamic membrane bioreactor–coagulation process. J. Petrol. Sci. Engineer. 74, 14–19.

Zhao, H., Chen, Q., Walker, N.D., Zheng, Q., MacIntyre, H.L., 2011. A study of sediment transport in a shallow estuary using MODIS imagery and particle tracking simulation. Int. J. Remote Sens. 32, 6653–6671.